# Time-Resolved Fluorescence Emission Measurements of Photosystem I Particles of Various Cyanobacteria: A Unified Compartmental Model

Bas Gobets,* Ivo H.M. van Stokkum,* Matthias Rögner,† Jochen Kruip,† Eberhard Schlodder,‡ Navassard V. Karapetyan,§ Jan P. Dekker,* and Rienk van Grondelle*

*Division of Physics and Astronomy of the faculty of Sciences and Institute of Molecular Biological Sciences, Vrije Universiteit, 1081 HV Amsterdam, The Netherlands; †Lehrstuhl Biochemie der Pflanzen, Ruhr-Universität Bochum, D-44780 Bochum, Germany; ‡Max-Volmer-Institut für Biophysikalische Chemie und Biochemie, Technische Universität Berlin, D-10623 Berlin, Germany; and §A.N. Bakh Institute of Biochemistry, Russian Academy of Sciences, Leninsky pr. 33, 117071 Moscow, Russia

ABSTRACT Photosystem I (PS-I) contains a small fraction of chlorophylls (Chls) that absorb at wavelengths longer than the primary electron donor P700. The total number of these long wavelength Chls and their spectral distribution are strongly species dependent. In this contribution we present room temperature time-resolved fluorescence data of five PS-I core complexes that contain different amounts of these long wavelength Chls, i.e., monomeric and trimeric photosystem I particles of the cyanobacteria *Synechocystis* sp. PCC 6803, *Synechococcus elongatus,* and *Spirulina platensis*, which were obtained using a synchroscan streak camera. Global analysis of the data reveals considerable differences between the equilibration components (3.4–15 ps) and trapping components (23–50 ps) of the various PS-I complexes. We show that a relatively simple compartmental model can be used to reproduce all of the observed kinetics and demonstrate that the large kinetic differences are purely the result of differences in the long wavelength Chl content. This procedure not only offers rate constants of energy transfer between and of trapping from the compartments, but also well-defined room temperature emission spectra of the individual Chl pools. A pool of red shifted Chls absorbing around 702 nm and emitting around 712 nm was found to be a common feature of all studied PS-I particles. These red shifted Chls were found to be located neither very close to P700 nor very remote from P700. In *Synechococcus* trimeric and *Spirulina* monomeric PS-I cores, a second pool of red Chls was present which absorbs around 708 nm, and emits around 721 nm. In *Spirulina* trimeric PS-I cores an even more red shifted second pool of red Chls was found, absorbing around 715 nm and emitting at 730 nm.

## INTRODUCTION

Photosystem I (PS-I) is one of two photosystems in oxygenic photosynthesis. It uses the energy of light to transfer electrons from plastocyanin or soluble cytochrome $c_6$ to $NADP^+$.

In plants and green algae, the PS-I complex consists of two distinct functional units: the PS-I core and the LHC I peripheral antenna. Although cyanobacterial PS-I lacks this peripheral antenna, their PS-I core complexes exhibit a strong homology to those of plants, and, therefore, the cyanobacterial PS-I can be used as a model system to study the energy and electron transfer dynamics in the core of PS-I (Cantrell et al., 1987; Mühlenhoff et al., 1993).

The PS-I core is a large protein complex consisting of at least 11 protein subunits, the largest two of which, PsaA and PsaB, form a heterodimer to which the largest fraction of the core antenna Chls and most of the reaction center (RC) co-factors are bound. Spectroscopic and structural data indicate that the core antenna and RC contain ~90 chlorophyll *a* (Chl*a*) and 10–25 $\beta$-carotene molecules in total (Krauss et al., 1996; Karapetyan et al., 1999).

*Received for publication 6 September 2000 and in final form 27 March 2001.*

Address reprint requests to Dr. Bas Gobets, Vrije Universiteit, Division of Physics and Astronomy, De Boelelaan 1081, 1081 HV Amsterdam, Netherlands. Tel.: 312-0447932; Fax: 312-20 4447899; E-mail: bas@nat.vu.nl.



0006-3495/01/07/407/18 $2.00

Recently, the structure of the PS-I core complex of the cyanobacterium *Synechococcus elongatus* was resolved with 4-Å resolution (Krauss et al., 1996; Fromme et al., 1996; Schubert et al., 1997). In this structure, 89 Chl molecules have been identified, including the 6 Chl*a* molecules that constitute the first part of the electron transfer chain in the RC. The 83 core antenna Chls were found to be arranged in a more or less elliptically shaped ring around the RC. The distance of most antenna Chls to any of the RC Chls was found to be larger than 20 Å. However, two antenna Chls, located at ~14 Å from the closest RC Chls, stood out in the structure, forming a structural, and possibly functional, bridge between the other antenna Chls and the RC. The six Chls in the RC constitute P700, a pair of accessory Chls, and the primary electron acceptor $A_0$. Also, other components of the electron-transfer chain, including the three $Fe_4S_4$ iron-sulphur clusters $F_x$, $F_A$, and $F_B$, could be assigned in the structure. Combining the structural data with single crystal EPR results allowed the localization of the two phylloquinones constituting $A_1$ (Klukas et al., 1999).

The ring-like organization of the antenna around the RC is a common feature in photosynthesis. The clearest example of such an arrangement is the light-harvesting I antenna of purple bacteria, which surrounds the RC. It can easily be shown that such an organization is a prerequisite for an efficient photosystem that includes a bulky RC. A system in which the RC is located in the center with a relatively large average distance to each antenna Chl, but in contact with many of them, is much more favorable than a system in

which the RC is located at the periphery of the antenna to which it is linked by only a few antenna Chls (Fleming and van Grondelle, 1997).

The cyanobacterial core complexes can be isolated both as monomers and trimers, and, because both are equally efficient in energy transfer and charge-separation (Turconi et al., 1996), it is not clear which is the native conformation; it may be that a dynamic equilibrium exists between monomers and trimers in the membrane that can be regulated by, for instance, the salt-concentration (Kruip et al., 1994). Energy transfer between the monomers within a trimer was found to be negligible at room temperature (Shubin et al., 1995).

## Low energy (red) chlorophylls

The PS-I core absorption spectrum is spectrally highly heterogeneous, and varies from species to species (van Grondelle et al., 1994). The absorption maximums of most of the core antenna Chls are distributed between 660 and 690 nm (bulk antenna) (Shubin et al., 1991; Wittmerhaus et al., 1992; van der Lee et al., 1993; Turconi et al., 1993; Gobets et al., 1994; Hastings et al., 1995; Turconi et al., 1996; see also below), which can be compared to the absorption maximum of isolated Chl*a* displaying a single broad maximum at ~662 nm in organic solvents (Hoff and Amesz, 1991). A conspicuous feature of all (intact) PS-I cores is the presence of a relatively small number of red shifted Chl states that absorb at energies lower than that of the primary electron donor P700. The amounts and energies of these low energy, or red, Chls appear to be highly species-dependent (Shubin et al., 1991; Wittmerhaus et al., 1992; van der Lee et al., 1993; Gobets et al., 1994; Pålsson et al., 1996; and below).

Based upon energy selective emission spectra of PSI, it has been proposed that the low energy Chls represent closely coupled dimers or larger aggregates of Chl*a* (Gobets et al., 1994).

In monomeric PS-I core preparations, the number of red Chls is generally found to be lower than in trimers. Especially the amplitude of the most red shifted Chl band may depend highly upon the aggregation state (Shubin et al., 1992; Pålsson et al., 1998). This effect suggests that at least some of these Chls are located in the periphery of the PS-I core, and that the red shift of these Chls may be induced by aggregation (Karapetyan et al., 1999).

At physiological temperatures the presence of the low energy Chls does not significantly decrease the quantum efficiency of charge separation. Even if these Chls are excited directly, thermal energy of the surrounding enables efficient uphill transfer to P700. At lower temperatures, however, the red Chls act as traps for excitations, thereby decreasing the quantum efficiency of charge separation (Pålsson et al., 1998; Trissl et al., 1993).

Although the low energy or red Chls only account for 2–10% of the total absorption of the core antenna, they do have a very pronounced effect on the fluorescence properties of the system. In *Synechocystis* core complexes with only two C708 red Chls (Gobets et al., 1994) the room temperature fluorescence emission spectrum exhibits a peak around 685–690 nm (F685) with a broad shoulder due to red Chls at ~710 nm. In contrast, in *Synechococcus* and *Spirulina* with more and longer wavelength absorbing red Chls (Pålsson et al., 1998; Shubin et al., 1992) the room temperature emission peaks above 700 nm, with F685 only appearing as a shoulder.

At low temperatures the emission from the red Chls fully dominates all fluorescence spectra, which peak at ~720 nm in *Synechocystis* (F720) and ~730 nm in *Synechococcus* trimers (F730). In trimers of *Spirulina* at low temperatures, one emission band is always present, peaking at ~730 nm (F730). A second emission band, with a maximum at ~760 nm (F760), may be observed depending on the oxidation state of P700: If P700 is pre-oxidized (using ferry-cyanide) F760 is absent, whereas it is present if the primary electron donor is reduced. The relatively strong spectral overlap of the F760 fluorescence with the absorption spectrum of $P700^+$, resulting in quenching of F760 emission, is thought to be the cause of this remarkable feature (Shubin et al., 1995). Monomeric PS-I cores of *Spirulina* only exhibit F730 fluorescence.

A decrease of the temperature also induces a dramatic increase of the fluorescence quantum yield of all PS-I particles (Gobets et al., 1994; Pålsson et al., 1998; Byrdin et al., 2000), due the trapping of excitations by the low energy Chls at low temperatures (see above).

## Energy transfer and trapping in PS-I

The core antenna of PS-I is intimately bound to the PS-I RC and, unlike in antenna-RC complexes of photosystem II and purple-bacterial photosystems, it is not possible to biochemically separate the core antenna from the RC. Therefore, time-resolved experiments on native PS-I have to be performed on systems with a large number (~100) of Chl*a* molecules which are all connected by energy transfer. Time-resolved spectroscopic experiments on such large antenna-RC complexes require the use of very low energy excitation pulses, to avoid the process of singlet-singlet annihilation (see for a review: Valkunas et al., 1995; van Grondelle, 1985).

Even if experiments are performed very carefully, the details of the processes that can be distinguished are limited. In an antenna-RC complex containing 100 Chl molecules, in principle 100 separate lifetimes are present in the excitation decay process. In reality, one can at best resolve a fraction of those lifetimes, but only if relatively selective excitation and detection is possible. Because the individual absorption and emission spectra of the 100 Chls in PS-I

cores are strongly overlapping, this condition of selectivity can only be met to a very limited extent, and consequently only a small number of (average) kinetic processes can be discerned.

The fastest processes that occur are single energy-transfer steps between two Chls. In PS-I cores, such single step transfer processes typically take place with time constants of a few 100 fs (Du et al., 1993; Kennis et al., 2001). Because the donor and acceptor Chls do not necessarily absorb at significantly different wavelengths, these steps may not be resolved in isotropic measurements. Anisotropic pump-probe or fluorescence up-conversion experiments can reveal energy transfer between iso-energetic Chls, provided that the absorbing and emitting dipole moments of donor and acceptor are not parallel.

As the Chls in PS-I absorb at different energies, energy redistribution processes take place due to which the initial distribution of excited antenna molecules transforms into a more thermally equilibrated distribution. Because the initial donor and final acceptor Chls absorb at different energies, equilibration appears as a decrease of fluorescence, or bleaching, in one part of the spectrum, and an increase in fluorescence or bleaching in another. It must be stressed that the observed equilibration lifetimes do not necessarily correspond to a one step energy transfer process, but generally reflect the net result of a (large) number of those steps. In PS-I core particles at room temperature, these equilibration components take place between the bulk antenna and the various pools of red Chls in the 2 to 15 ps time-range (Holzwarth et al., 1993; Turconi et al., 1993; Hastings et al., 1994; Hastings et al., 1995; Turconi et al., 1996; Karapetyan et al., 1997; Savikhin et al., 1999a; Melkozernov et al., 2000; Byrdin et al., 2000; and see below), and within the bulk antenna on a sub-ps time scale (Savikhin et al., 1999a; Melkozernov et al., 2000; Kennis et al., 2001). In order to accurately record these processes, high time-resolution, and spectrally resolved techniques are required such as multi-colour pump-probe, fluorescence up-conversion, or streak-camera fluorescence detection.

The slowest components that are observed are the so-called trapping components, which represent the overall rate at which excitations disappear from the system by charge separation in the RC, following equilibration processes that may have occurred in the antenna on a shorter time scale (see above). In time-resolved fluorescence spectroscopy experiments, trapping appears as the slowest rate of the system with a decay of fluorescence at all wavelengths of detection. In pump-probe transient absorption experiments trapping is observed as the rate at which the spectrum of $P700^+$ is formed, which generally lives infinitely on the time scale of these experiments. Because the trapping component typically has a lifetime of tens of ps, it can be recorded quite accurately, even with moderate time-resolution techniques such as single photon timing (SPT) (van Grondelle et al., 1994).

During the past decade PS-I of a wide variety of species has been studied by several groups using (sub)picosecond time-resolved spectroscopic techniques including pump-probe (Holzwarth et al., 1993; Hastings et al., 1994, 1995; Pålsson et al., 1995; Savikhin et al., 1999a; Melkozernov et al., 2000), SPT (Holzwarth et al., 1993; Turconi et al., 1993; Hastings et al., 1994; Turconi et al., 1996; Karapetyan et al., 1997; Byrdin et al., 2000) and fluorescence up-conversion (Du et al., 1993; Kennis et al., 2001). Various rate constants have been found for the energy redistribution within the main antenna, between main antenna Chls and red Chls, and trapping in the RC. It has been suggested (Hastings et al., 1995) that the variability of the results is more likely due to experimental differences rather than to real variation between the investigated species. To clarify this point we have decided to investigate the dynamics of different PS-I cores of a number of cyanobacteria under identical experimental conditions. These time-resolved fluorescence experiments were performed using a synchroscan streak-camera with a spectrograph which has an instrumental response of $\sim$3 ps and enables us to observe kinetics occurring significantly faster than 1 ps. In all studies referred to above, either time traces were measured sequentially for different detection wavelengths, or spectra were measured sequentially for different delay times. In contrast to this, our setup integrates spectral and temporal data simultaneously resulting in high quality spectra which allow quantitative analysis.

It will be shown that the experimentally observed kinetics are indeed quite different between the five PS-I particles studied. However, we will clearly demonstrate that the dynamics in all these PS-I cores are essentially the same, and that the observed differences are resulting entirely from differences in the amounts and energies of the red Chls present in the various PS-I cores.

## MATERIALS AND METHODS

The *Synechocystis* sp. PCC 6803 PS-I monomers and trimers were prepared as in Kruip et al. (1993), the trimeric PS-I complexes from the thermophilic cyanobacterium *S. elongatus* were isolated as in Fromme and Witt (1998) and monomeric and trimeric PS-I particles from *Spirulina platensis* were prepared as described in Kruip et al. (1999).

For the fluorescence experiments the concentrated samples were diluted to an $OD_{680}$ of 0.6/cm with a buffer containing 20 mM $CaCl_2$, 20 mM $MgCl_2$, 10 mM 2-(*N*-morpholino)ethane sulfonic acid, and 0.05% w/v dodecyl-$\beta$-D-maltoside at a pH of 6.5 (*Synechocystis* and *Synechococcus*) or 10 mM $CaCl_2$, 10 mM $MgCl_2$, 10 mM Tris-HCl and 0.03% w/v dodecyl-$\beta$-D-maltoside at a pH of 7.8 (*Spirulina*). Ten mM sodium ascorbate and 10 $\mu$M phenazine meta sulphate were added to all samples to avoid accumulation of $P700^+$.

To avoid multiple excitation of the sample by successive laser flashes it was contained in a spinning cell (diameter, 10 cm) rotating at 20 Hz. All experiments were performed at room-temperature (293 K).

The samples were excited using 100 to 200-fs pulses at 400 nm, which were generated at a 100 kHz repetition rate using the frequency-doubled output of a laser system consisting of a titanium/sapphire based oscillator (Coherent MIRA) and a regenerative amplifier (Coherent REGA). The excitation light was collimated with a 15 cm focal length lens, resulting in

a focal diameter of 150 $\mu$m in the sample. Fluorescence was collected at right angle to the excitation using achromatic lenses and detected through a sheet polarizer set at magic angle (54.7°) with a Hamamatsu C5680 synchroscan streak camera and a Chromex 250IS spectrograph. The streak images were recorded on a Hamamatsu C4880 CCD camera which was cooled to −55°C.

The full width at half of the maximum of the overall time response of this system was 3–3.5 ps. The spectral resolution was 8 nm. One streak image measured 315 nm in the spectral domain (1018 pixels) and 200 ps (1000 pixels) in the time domain.

To avoid singlet-singlet annihilation, the pulse energy was reduced to 1 nJ, thus exciting typically only 0.25% of all Chls present in the focus.

The pathlength of the recorded fluorescence emission through the setup is wavelength-dependent, resulting in a wavelength-dependent position of time 0 on the streak image. This time dispersion was assessed by recording the streak image of a (pulsed) white-light continuum which was scattered in a dilute solution of coffee creamer, and combining this data with the intrinsic time dispersion of this white-light continuum which was obtained in a pump-probe measurement of $CS_2$ (Greene and Farrow, 1983).

Before the global analysis the streak images were background-subtracted and corrected for difference in sensitivity in the time domain by division by a streak image of a halogen lamp (shading correction). Subsequently the dispersion correction was applied, and the relevant spectral region of the image was divided in 30−60 traces by spectral integration over 3–5 nm.

In the global analysis fitting a Gaussian shaped instrument response function was assumed. The width of this Gaussian was a free parameter of the fit (typically 3.5 ps). In some cases the fit was improved by allowing for a small additional contribution (~5%) of a broader Gaussian to the instrument response.

All measurements were analyzed using a model with a number of parallel compartments, which yields decay-associated spectra (DAS). The periodicity of the synchroscan with a period of 13.4 ns results in a back and forth sweeping of long lived (>1 ns) components. By taking this into account in the fit, the lifetime and spectrum of a (single) long-lived component (such as some free Chl present in the sample) could be estimated accurately on the 200-ps time scale.

All of the DAS shown were corrected for the spectral sensitivity of the apparatus.

The quality of the fit was judged by the root mean square error and by examination of the residual matrix with the help of singular value decomposition to extract the temporal and spectral structure (Hoff and Amesz, 1994).

The target analysis (Holzwarth, 1996) yielded the species associated emission spectra (SAES) of the different pools of red Chls. In order to obtain these spectra a constraint had to be put on the SAES of the long wavelength Chls which were put to zero at wavelengths shorter than ~680 nm (1st pool) and ~690 nm (2nd pool).

## RESULTS

### Absorption spectra

In Fig. 1 the 6-K absorption spectra of the various investigated PS-I particles are displayed. In the region below 700 nm, the spectra of all particles are very similar, consisting of a large absorption band with a maximum at 680 nm and a shoulder around 673 nm. This spectral region is dominated by the absorption of the bulk antenna Chls, which comprise 90% or more of the total Chl content. Pronounced differences between the various PS-I species are observed only in the region above 700 nm, where the absorption of a relatively small number of red Chls dominates the spectra. As

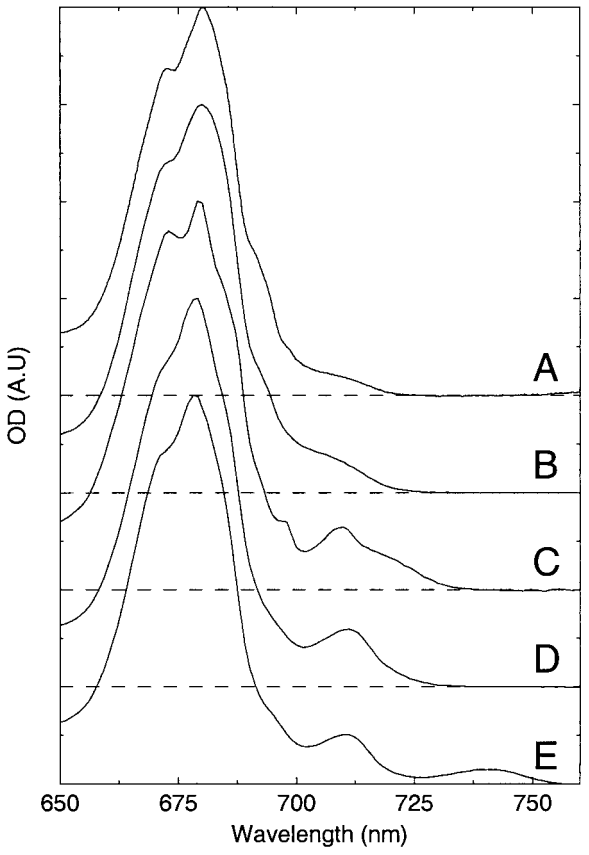


FIGURE 1 6 K absorption spectra of different cyanobacterial PS-I core particles. (*A*) Monomeric core of *Synechocystis sp.* PCC 6803. (*B*) Trimeric core of *Synechocystis sp.* PCC 6803.(*C*) Trimeric core of *Synechococcus elongatus*. (*D*) Monomeric core of *Spirulina platensis*. (*E*) Trimeric core of *Spirulina platensis*.

the absorption bands of red Chls are quite distinct at 6 K, the maximums of these bands and the number of Chls contained in them can be estimated by Gaussian deconvolution of the absorption spectra.

The spectrum of monomeric PS-I core particles from *Synechocystis* (Fig. 1 *A*) reveals an inhomogeneously broadened absorption band with a maximum at 708 nm (C708). This band was found to carry an oscillator strength of approximately 2 Chl*a* molecules (Gobets et al., 1994). This estimation was based on a total number of 65 Chls in the core antenna. Because the true number of antenna Chls is probably closer to 100, we now estimate the number of C708 Chls in *Synechocystis* monomeric PS-I to be close to 3. The spectrum of PS-I trimers from *Synechocystis* (Fig. 1 *B*) resembles the one reported by Rätsep et al. (2000) and exhibits significantly more long wavelength absorption than monomeric PS-I from this species. Hayes et al. (2000) suggested that two Chls contribute to C706, and two other Chls contribute to C714. We note, however, that the suggestion of Hayes et al. (2000) that these pools are connected by energy transfer is at odds with the site-selected emission

measurements of Gobets et al. (1994) on trimeric PS-I particles from *Synechocystis*. From the 6-K OD spectrum of PS-I trimers from *Synechocystis* we estimate that a total number of 4 to 5 C708 are present in these PS-I cores. The exact number of C708 Chls in this species, however, seems to vary somewhat between different isolations.

Two red absorption bands are found in the 6K absorption spectrum of the trimeric core particles of *Synechococcus* (Fig. 1 *C*) with maximums at 708 nm (C708, corresponding to 4–5 Chl*a*s) and 719 nm (C719, corresponding to four Chl*a*s) (Pålsson et al., 1996). The monomers show a 50% reduction of C719 (not investigated in this study) (Pålsson et al., 1998).

The monomeric complexes of *Spirulina* (Fig. 1 *D*) exhibit a dominant absorption band at 708 nm corresponding to ~7 Chls and a minor contribution of C719 (~1 Chl). The latter contribution is not very clear, and may also reflect a tail of a single band of red Chls that exhibits a large and asymmetric inhomogeneous distribution. Trimeric PS-I cores of *Spirulina* (Fig. 1 *E*) exhibit an absorption band at ~708 nm which is similar to the one found in monomers (C708, corresponding to ~7 Chl*a*) but also display an absorption band with a maximum at 740 nm (C740, corresponding to ~3 Chl*a*), which constitutes the redmost absorbing species reported in any PS-I complex. (Shubin et al., 1992; Karapetyan et al., 1997, 1999). The assignments and sizes of the red Chl pools for the various PS-I species are summarized in Table 1.

For comparison the red parts of the room temperature absorption spectra for the various PS-I cores are shown in Fig. 2. At room temperature the red Chls only appear as a long, featureless red tail to the absorption spectrum. Nevertheless, some features are still visible. The PS-I cores of *Synechocystis* monomers (*solid*) show the least red absorption. PS-I trimers of *Synechocystis* (*dashed*) show slightly more red absorption, but still much less than the other three PS-I particles. *Synechococcus* trimeric PS-I (*dotted*) and *Spirulina* monomeric PS-I (*long dashed*) show a very similar red wing, although the latter appears to be slightly blue shifted as compared to the former. *Spirulina* trimeric PS-I also at room-temperature exhibits the most red-extended absorption of all studied PS-I particles.

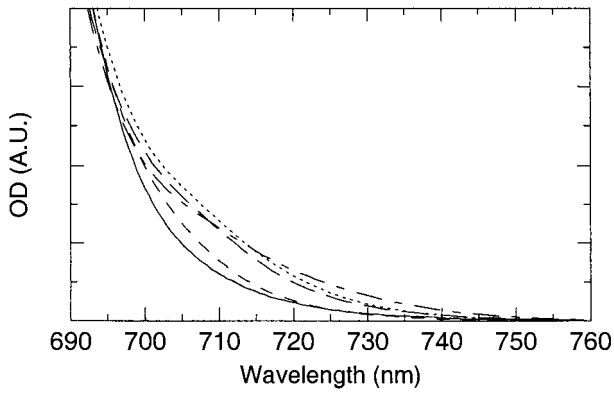


FIGURE 2 The red region of the room-temperature absorption spectra of monomeric core of *Synechocystis sp.* PCC 6803 (*solid line*), trimeric core of *Synechocystis sp.* PCC 6803 (*dashed line*), trimeric core of *Synechococcus elongatus* (*dotted lines*), monomeric core of *Spirulina platensis (long dashed lines)*, and trimeric core of *Spirulina platensis* (*dashed-dotted lines*). The spectro were normalized at the Qy absorption maximum.

## Time-resolved fluorescence measurements

We have recorded the time-resolved fluorescence kinetics of five different PS-I preparations upon excitation at 400 nm, all under essentially identical conditions. In Fig. 3 we show typical time-resolved fluorescence traces of the *Spirulina* trimers for two different wavelengths of detection. The raw data (*noisy solid*) and the fit (*smooth solid*) are shown along with the different lifetime contributions obtained in the global analysis of the data (*dashed with markers*). We note that the global analysis involved a total of 30 to 60 wavelengths of detection.

Comparing the raw data for detection at 684 nm (Fig. 3 *A*) and 745 nm (Fig. 3 *B*) reveals some clear differences: the trace at 684 nm, which mainly represents the emission from the bulk Chls, has a very distinct maximum in time, whereas

**TABLE 1 6K and room temperature low energy Chl*a* absorption and emission**

| | First pool (C708) | | | | | Second pool (C719, C740) | | | | |
|---|---|---|---|---|---|---|---|---|---|---|
| | Absorption (nm) | | Emission (nm) | | No. | Absorption (nm) | | Emission (nm) | | No. |
| Species | 6 K | RT | 6 K | RT | chls/100 | 6 K | RT | 6 K | RT | chls/100 |
| *Synechocystis* monomers | 708 | 703 | 720 | 712 | ~3 | | | | | |
| *Synechocystis* trimers | 708 | 702 | 720 | 711 | ~5 | | | | | |
| *Synechococcus* trimers | 708 | 702 | | 707 | ~5 | 719 | 708 | 730 | 723 | ~4 |
| *Spirulina* monomers | 708 | 699 | | 712 | ~7 | 719 | 719 | 730 | 721 | ~1 |
| | | (702) | | | (5) | | (708) | | | (3) |
| *Spirulina* trimers | 708 | 703 | | 714 | ~7 | 740 | 715 | 760 | 733 | ~3 |

Except for the values in parenthesis, the 6K absorption properties of the low energy Chls were estimated from a Gaussian deconvolution of the absorption spectra. Room temperature absorption and emission properties were obtained from the target analysis of the time-resolved fluorescence data. For details, see text.

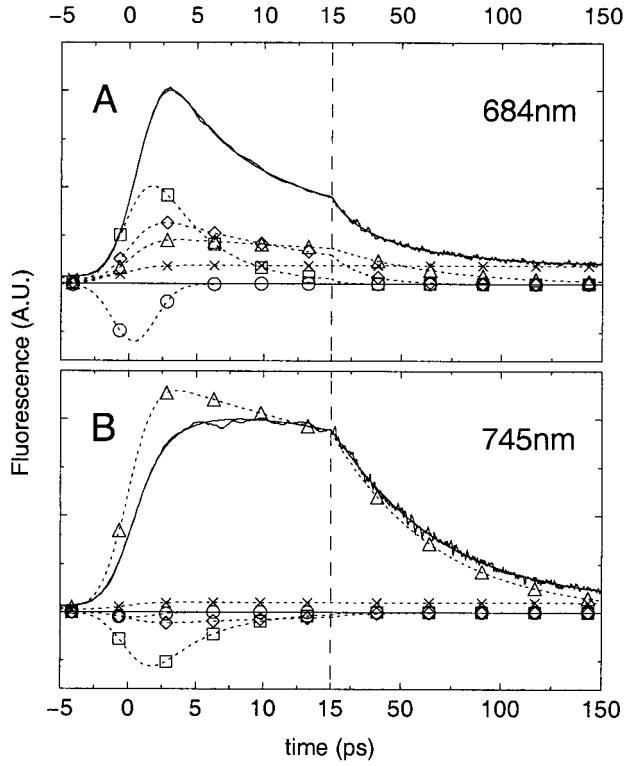


FIGURE 3 Time-resolved fluorescence traces of *Spirulina* trimeric PS-I detected at 684 nm (*A*) and 745 nm (*B*), for excitation at 400 nm. Data and fit are represented by *solid lines*; *dashed lines* with markers represent contributions of different lifetime components (*circles*, 0.4 ps; *squares*, 3.9 ps; *diamonds*, 15 ps; *triangles*, 50 ps; *crosses*, 5 ns). Note the change of the scaling of the time axis at 15 ps.

the trace at 745 nm, which mainly represents emission from the red Chls, does not exhibit such a well-defined maximum; the amplitude appears to be almost constant between 5 and 15 ps after excitation. At times later than 15 ps, the kinetics for both detection wavelengths are very similar, decaying almost mono-exponentially to a constant value. The observed differences during the first 15 ps of both traces reflect the energy transfer from the bulk Chls emitting around 684 nm to the red Chls emitting around 745 nm, which causes a rapid initial decrease of the fluorescence at 684 nm, and a simultaneous increase of the fluorescence at 745 nm.

The various lifetime contributions which were estimated by a global analysis fitting procedure (Fig. 3, *dashed with markers*), display this process in more detail. For 684 nm detection (Fig. 3 *A*) all contributions but one [the 400 fs component (*circles*) reflecting Soret-$Q_y$ relaxation, see below] show a positive amplitude expressing a decay of fluorescence. The analysis demonstrates that the decay includes significant contributions by a 3.9 ps (*squares*) and a 15 ps (*diamonds*) lifetime component, which account for most of the dynamics observed in the first 15 ps after excitation. For 745-nm detection (Fig. 3 *B*) the rapid decay during the first 15 ps after excitation is not present because the 3.9- and 15-ps contributions show a negative amplitude at this wavelength of detection, expressing an increase of fluorescence with these time constants. Because the 3.9- and 15-ps components show a decay at 684 nm and a rise at 745 nm, these components reflect energy transfer from the bulk Chls to the red Chls. The 50-ps component (*triangles*), which is positive for both wavelengths of detection, reflects the overall decay of excitations from the system (trapping component). The small 4.9-ns contribution (*crosses*), which is positive at both wavelengths of detection, can be attributed to a small fraction of uncoupled Chls present in the preparation. Results qualitatively very similar to those shown in Fig. 3 were obtained for all PS-I species investigated in this study.

## Global analysis

We will now discuss in more detail the results of the global analysis of the data obtained for all PS-I species studied and for all wavelengths of detection. The decay associated spectra of the measurements of the 5 different PS-I core particles are presented in Figs. 4 *A–E*. All spectra have been scaled to the total number of excitations, and therefore not only the shapes, but also the amplitudes of the various components can be compared directly.

In all preparations a small decay component is found with a lifetime of about 5 ns, that was already mentioned with reference to Fig. 3 (Fig. 4 *A–E*, *crosses*). The lifetime of these components and the corresponding spectra, which peak at 675–678 nm and exhibit a long tail in the red region, are indicative of Chl*a* in solution. We therefore assign these components to a fraction of Chls in the preparation that is not attached to the protein. Hence, these components do not express a process in the intact systems.

### *Monomeric and trimeric PS-I from* Synechocystis *sp. PCC* 6803

With 400-nm light, initially the Soret band, a higher electronic state of Chl*a*, is excited. This state relaxes to the lowest singlet excited Chl*a* state ($Q_y$) in a few hundred fs, like found for BChl (Limantara et al. 1998). Therefore the fluorescence in the $Q_y$ region does not appear instantaneously, but rises with a finite time-constant. In all PS-I particles investigated in this study this is evident from a sub-picosecond component which exhibits an all-negative DAS (Fig. 4 *A–E*, *circles*). This ingrowth is not observed for direct excitation in the $Q_y$ region (data not shown). For *Synechocystis* monomeric PS-I the lifetime of this component is fitted by a 0.8 ps lifetime (Fig. 4 *A*, *circles*).

The second component in monomeric PS-I from *Synechocystis* exhibits a lifetime of 4.4 ps and is represented by a DAS which is positive at short wavelengths with a distinct maximum around 686 nm, crosses zero at ~701 nm, and

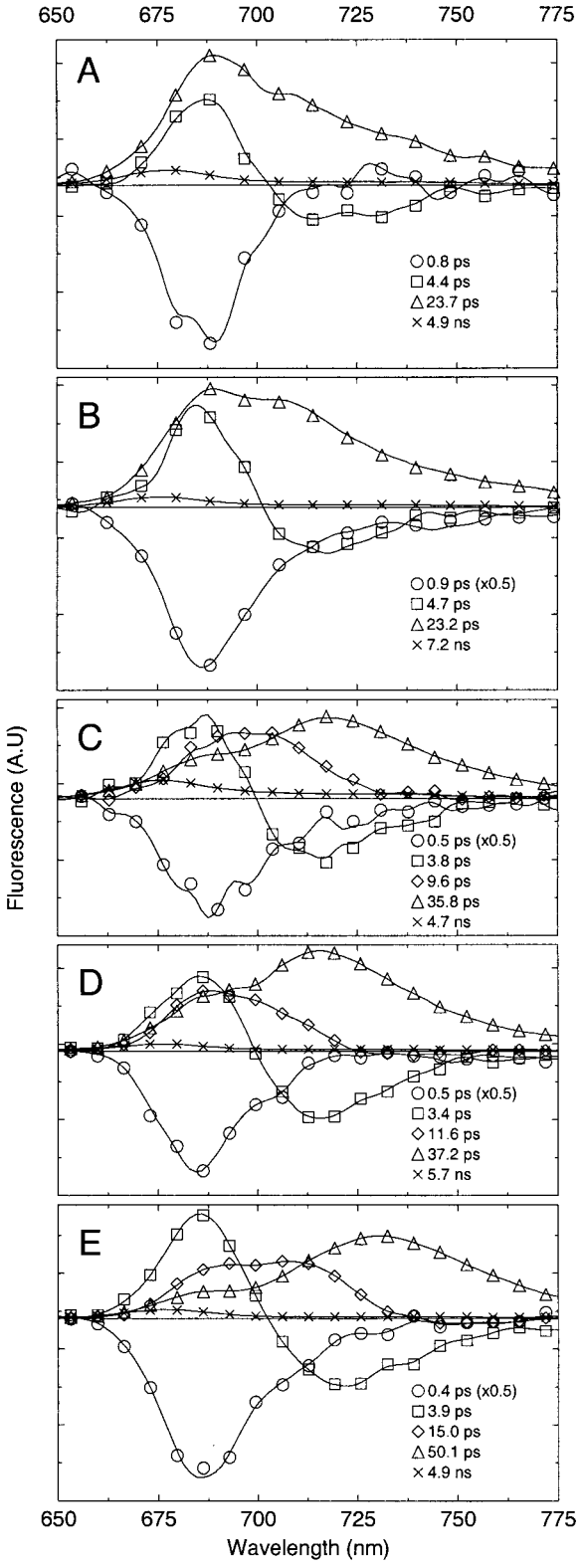


FIGURE 4 Decay Associated Spectra of fluorescence decay of different cyanobacterial PS-I core particles upon excitation at 400 nm. (*A*) Monomeric core of *Synechocystis sp.* PCC 6803. (*B*) Trimeric core of *Synechocystis sp.* PCC 6803. (*C*) Trimeric core of *Synechococcus elongatus* (*D*) Monomeric core of *Spirulina platensis*. (*E*) Trimeric core of *Spirulina platensis.* For clarity only one marker is shown for every two data points.

exhibits a shallow negative region above this wavelength (Fig. 4 *A*, *squares*). PS-I from *Synechocystis* probably exhibits only one pool of long wavelength Chls, peaking at 708 nm at 6 K (see above), and the 4.4-ps component displays the net downhill energy transfer from the bulk Chls to this pool of long wavelength Chls, reflecting the relaxation of the initially excited Chl distribution into a thermally more equilibrated distribution.

This equilibration spectrum is clearly not conservative: the area above zero is significantly larger than the area below. This shows that the spectrum is not a pure equilibration spectrum, but that also some (fast) trapping from the non-equilibrated state occurs during the equilibration process. Thus, the observed spectrum is the sum of a conservative pure equilibration contribution and a trapping contribution that is positive at all wavelengths. This feature can be reproduced both by simple compartmental models (see below) and by structure-based simulations (Gobets et al., 1998a,b).

The final component in monomeric PS-I from *Synechocystis* is represented by a DAS that is clearly positive at all wavelengths of detection and exhibits a lifetime of 23.7 ps, this being the longest lifetime actually occurring in the system (the ns lifetime is not due to intact systems, see above). Such a component is generally referred to as the trapping component of the system: the spectrum does not change any more, and decays with one single time-constant. The trapping DAS of *Synechocystis* monomeric PS-I peaks at 688 nm (Fig. 4 *A*, *triangles*), reflecting dominant emission from the bulk Chls. The presence of the few red Chls in this PS-I species is revealed by a shoulder in the spectrum around 708 nm.

To distinguish between transfer components which may also incorporate some non-equilibrium trapping, and the trapping component as defined above, we will continue to refer to the former as equilibration or energy transfer components.

The results for trimeric PS-I particles from *Synechocystis* (Fig. 4b) are very similar to those found for monomers. The lifetimes do not differ significantly, and the DAS only display slight (but significant) differences. The ingrowth from the Soret is fitted with a 900-fs lifetime. The equilibration component is fitted with a 4.7 ps time-constant (Fig. 4, *A* and *B*, *squares*) and the amplitude of the corresponding DAS is significantly higher in the trimers as compared to the monomers. Trapping in trimeric PS-I of *Synechocystis* occurs in 23.2 ps and the corresponding spectrum (Fig. 4 *B*, *triangles*) differs from that of monomers by a more pronounced shoulder around 708 nm. Both the enhanced amplitude of the downhill transfer component and the rise of the shoulder reflect the higher red Chl content of the PS-I trimers of *Synechocystis* as compared to monomers (Gobets et al., 1994; Rätsep et al., 2000).

The lifetimes of the equilibration components found in this study correspond reasonably well with earlier SPT

experiments (Hastings et al., 1994; Turconi et al., 1996) and pump-probe experiments (Hastings et al., 1994, 1995) performed on *Synechocystis* PS-I, in which equilibration upon aselective excitation was found to occur in 5 and 3.7 ps respectively. Recent pump-probe experiments performed on trimeric PS-I cores from *Synechocystis* (Savikhin et al., 1999a) reveal a 4.8-ps component as well, although the authors also present a better fit of their data using two equilibration components with lifetimes 2 and 6.5 ps, respectively. In another recent pump-probe studies on a mixture of PS-I monomers and trimers from *Synechocystis* (Melkozernov et al., 2000) equilibration is found to occur in ~2.3 ps. In our data there is no evidence of a (second) fast equilibration process occurring in ~2 ps. Of course, the time-resolution of the streak camera is less as compared to the above-mentioned pump-probe experiments, but the apparent discrepancy of our results with these experiments could also be due to the use of too high excitation powers in the latter, resulting in singlet-singlet annihilation which introduces non-physiological and non-exponential decay components (Valkunas et al., 1995; van Grondelle, 1985). Savikhin et al. (1999a) show a power dependence of a trace at 700 nm, but because there is still some difference between the lowest and the one-but-lowest energy trace, this does not convincingly rule out annihilation. Also, their estimate of exciting one out of every 120 Chls would imply that with each laser shot, about one-third of the excited PS-I complexes would receive more than one excitation, resulting in annihilation (estimated using Poisson statistics, and 100 Chls/PS-I, assuming no significant amount of energy transfer between monomers in a trimer). The 1–3 nJ/pulse reported by Melkozernov et al. (2000) could be relatively safe, although they do not specify the spot size of the focus of the excitation light. (In fact, they state a pulse energy of 1–3 $\mu$J/pulse, but this must certainly be 1–3 $\mu$W at a 1-kHz rep rate).

The lifetime and spectrum of trapping are consistent with earlier measurements on *Synechocystis* PS-I (Turconi et al., 1996; Hastings et al., 1994, 1995; Savikhin et al., 1999a; Melkozernov et al., 2000).

### *Trimeric PS-I particles from* S. elongatus

The fluorescence DAS of trimeric PS-I from *Synechococcus* following 400 nm excitation are shown in Fig. 4c. In this species the Soret $Q_y$ relaxation also represents the fastest process, which is fitted with a 500-fs lifetime (Fig. 4 *C*, *circles*).

For *Synechococcus* PS-I trimers, which, in contrast to *Synechocystis* PS-I, contain 2 pools of long wavelength Chls (C708 and C719), two separate energy transfer components of 3.8 and 9.6 ps can be distinguished (Fig. 4 *C*, *squares* and *diamonds*). The 3.8-ps equilibration component exhibits a DAS of which the positive region displays a shape and amplitude which are very similar to the equilibration DAS of *Synechocystis* PS-I, showing a maximum around 686 nm, and a zero crossing at 700 nm. The negative part is deeper however, and shows a pronounced minimum around 715 nm. The spectrum is more or less conservative, indicating that in the trimeric PS-I core of *Synechococcus* the amount of trapping occurring with the 3.8-ps time-constant is negligible.

In contrast to the 3.8-ps equilibration component, the 9.6-ps component DAS is highly non-conservative and basically consists of a broad positive contribution peaking around 700 nm. The DAS is about zero above ~730 nm, but does not become distinctly negative. This shows that a significant amount of trapping occurs during the 9.6-ps process. The lack of a clear negative part in the spectrum does not imply that this spectrum is a pure trapping spectrum: the sum of an all positive pure trapping contribution and a conservative pure transfer component can easily be positive at all wavelengths. The differences between the 3.8- and 9.6-ps DAS indicate that in this PS-I species energy transfer between the bulk antenna Chls and the first (C708) pool of long wavelength Chls occurs on a fast time scale, and that the energy transfer from bulk Chls and C708 to more red shifted Chls takes place on a slower time scale.

So far, these two distinct equilibration components have not been observed separately. In an early combined SPT pump-probe study (Holzwarth et al., 1993) only one equilibration component was revealed with a time-constant of 8–12 ps (depending on the technique applied), although the authors suggested the existence of another unresolved energy transfer contribution. The spectrum of this single 8- to 12-ps component exhibited both pronounced positive and negative areas, and is therefore quite different from the weighted sum of the two equilibration spectra that were found in our experiments. We note that in particular this phenomenology recorded by Holzwarth et al. (1993) was at the basis of the extensive modelling by Trinkunas and Holzwarth (1994). Also, in a very recent SPT study (Byrdin et al., 2000) only one energy transfer component was observed, which had a lifetime of 13 ps, and a spectrum that showed a negative area which was much larger than the positive area, in clear contradiction with both our measurements, and those by Holzwarth et al. (1993).

The final component is fitted with a 35.8-ps time-constant, and represents trapping from the equilibrated distribution of excitations (Fig. 4 *C*, *triangles*). *Synechococcus* PS-I trimers do not only contain a considerably larger number of red Chls but about half of them also appear at lower energies than in *Synechocystis* (Fig. 1 *C* and Table 1). As a consequence the maximum of the trap spectrum is shifted to 719 nm, reflecting a dominant contribution of fluorescence from the red Chls. The fluorescence of the bulk Chls only appears as a shoulder around 690 nm.

The observed trapping lifetime and spectrum are consistent with the earlier results by (Holzwarth et al., 1993; Byrdin et al., 2000).

*Monomeric and trimeric PS-I from* Sp. platensis

In PS-I monomers of *Spirulina*, the ingrowth from the Soret state is fitted with a 500-fs lifetime (Fig. 4 *D*, *circles*), and the subsequent events include two equilibration processes taking place in 3.4 and 11.6 ps, respectively (Fig. 4 *D*, *squares* and *diamonds*). The 3.4-ps component peaks at 685 nm, has a zero crossing at 699 nm, exhibits a distinct minimum at 715 nm and is more or less conservative. The lifetime, spectral shape and amplitude of this component are virtually identical to the 3.8-ps component found in trimeric PS-I of *Synechococcus*.

The DAS of the 11.6 ps equilibration component consists of a broad band positive contribution which peaks at ~688 nm, significantly more to the blue than the corresponding DAS in *Synechococcus* PS-I. In contrast to the second equilibration DAS of *Synechococcus* PS-I which does not exhibit a real negative region, the 11.6 ps DAS in *Spirulina* monomeric PS-I slightly drops below zero above ~728 nm. Nevertheless this component is highly non-conservative, indicating that also in this species a significant amount of non-equilibrium trapping occurs during the second equilibration process. It seems obvious to associate the occurrence of two equilibration components in *Spirulina* monomeric PS-I with the presence of two distinctly different Chl pools. An alternative could be, however, that the long wavelength region in *Spirulina* monomers does not consist of two distinctly different pools, but rather of a single (large) C708 pool which exhibits an exceptionally broad inhomogeneous distribution. (as suggested above in the discussion of the 6-K absorption spectra). In this view the two distinct equilibration components that are observed may simply reflect the two-pool approximation of a broad distribution of lifetimes and spectra.

The trapping lifetime of 37.2 ps and the corresponding spectrum in *Spirulina* monomers (Fig. 4 *D*, *triangles*) are very similar to that of *Synechococcus* PS-I trimers. The spectrum peaks only slightly more blue (at 715 nm) than the latter (719 nm), and exhibits a slightly higher shoulder at 690 nm. These small differences reflect that, although the total amount of red Chls in both species is comparable, their absorption is on the average slightly more blue in *Spirulina* monomeric PS-I as compared to *Synechococcus* trimeric PS-I (see above).

Our general observation is that all lifetimes and spectra found in *Spirulina* PS-I monomers are remarkably similar to those found in *Synechococcus* PS-I.

In contrast to PS-I from *Synechocystis*, the results of monomeric and trimeric PS-I of *Spirulina* differ very significantly (Fig. 1 *D* and *E*, Fig. 4 *D* and *E*). The 6-K absorption spectrum of trimeric PS-I complexes from *Spirulina* clearly exhibits two distinct pools of long wavelength Chls (see above); in addition to the C708 pool, which occurs throughout all PS-I complexes investigated in this studies, trimeric PS-I from *Spirulina* also exhibits an extremely red shifted C740 pool that is not present in monomeric PS-I of this species. For trimeric PS-I from *Spirulina* the ingrowth from the Soret state is fitted with a 400-fs lifetime (Fig. 4 *E*, *circles*).

In the kinetics of *Spirulina* trimeric PS-I two equilibration components can be distinguished, occurring with time constants of 3.9 and 15 ps (Fig. 4 *E*, *squares* and *diamonds*), both slightly slower than found in the monomeric PS-I complexes of this species.

The fast 3.9-ps DAS displays a shape which at first glance appears quite similar to the 3.4-ps DAS found in monomers. The amplitude is somewhat higher for trimers, however, and the zero crossing and the minimum of the spectrum are both significantly red shifted to 703 and 722 nm, respectively.

The 15-ps DAS, which represents the second equilibration process, clearly displays more significant differences with the monomers. In the trimer the spectrum of this component is also highly non-conservative, but in contrast to the monomers, the positive region clearly displays a double peaked structure, with maximums at ~691 and ~706 nm. The zero-crossing is located at about 740 nm, and the negative region at longer wavelengths is more pronounced than the corresponding DAS in monomers.

Trapping in *Spirulina* PS-I trimers is by far the slowest of all the PS-I species we investigated, at 50 ps. Due to the extremely red shifted Chl forms that occur in *Spirulina* PS-I trimers, they exhibit a trapping DAS that is very red shifted, showing a maximum at 730 nm. The contribution of the bulk Chls to this DAS is small, as reflected by the very low shoulder around 688 nm.

An earlier, time-resolved emission study (Karapetyan et al., 1997) revealed one single 9-ps equilibration component as well as two all positive components with lifetimes of 28 to 31 ps and 65 to 69 ps, both in PS-I monomers and trimers of *Spirulina*. The differences with our observations can most probably be ascribed to the much lower time-resolution of the earlier study, which may have caused some mixing of the different components, because all observed time constants are either equal to or significantly faster than the instrument response of the setup used by (Karapetyan et al., 1997).

## DISCUSSION

### Global analysis

*Soret-$Q_y$ relaxation*

As mentioned in above, in the time-resolved fluorescence experiments presented here, initially the Soret band, a higher electronic state of Chl*a*, is excited, which relaxes to the lowest singlet excited Chl*a* state ($Q_y$) in a few hundred fs. Although the instrument response of the streak camera is significantly longer than this relaxation process, it can clearly be distinguished, which is mostly due to the accu-

rately determined (~100 fs) relative position of time 0 for the different wavelengths of detection. The Soret $Q_y$ relaxation is evident from an all-negative DAS, which is present in the kinetics of all PS-I particles studied (Fig. 4 *A–E*, *circles*). The fitted lifetime of the relaxation varies between 0.4 and 0.9 ps, but in view of the instrument response of our setup this variation is not significant. All fitted lifetimes are probably somewhat slower than the actual lifetime of Soret-$Q_y$ relaxation.

Because the Chl*a* molecules are excited aselectively at 400 nm, independent of their $Q_y$ absorption maximum, and because most likely the major part of the energy transfer occurs after Soret-$Q_y$ relaxation, the ingrowth spectra are expected to resemble the $Q_y$ region of the OD spectra (after changing the sign of the spectrum and taking into account an average Stokes' shift). The spectra corresponding to the rise (Fig. 4 *A–E*, *circles*) indeed show a spectral shape similar to that of the OD spectrum in the $Q_y(0-0)$ absorption region. The minima of the ingrowth spectra occur between 685 and 689 nm, suggesting a value of the Stokes' shift of 5 to 9 nm for the bulk antenna Chls, which may be compared to the ~7 nm Stokes' shift found for Chl*a* in solution (Hoff and Amesz, 1991). A Stokes' shift of 6.5 nm was also found for the single Chl*a* in the cytochrome $b_6f$ complex from *Synechocystis* (Peterman et al., 1998). These results suggest that in PS-I no significant red shift of the emission spectrum occurs in the first few hundred femtoseconds.

The amount of carotenoids excited at 400 nm is <10%, as estimated from a comparison with an experiment in which the carotenoids were excited directly at 510 nm (results not shown). Because most of the transfer from the carotenoids to the Chls occurs on a timescale comparible to the Soret $Q_y$ relaxation (Kennis et al., 2001), the small fraction of carotenoids excited at 400 nm will have no significant effect upon our results.

### *Energy transfer components*

Because all experiments were performed under magic-angle conditions, no single step transfer kinetics between isoenergetic Chls could be discerned, because these ultra-fast equilibration components can only be observed by high time-resolution anisotropic experiments. Also equilibration between spectrally different Chls in the bulk antenna is not observed for this wavelength of excitation.

We do however observe components that are represented by a DAS which is positive at relatively short wavelengths and negative in the region of red Chl emission (Fig. 4 *A–E*, *squares* and *diamonds*), and which reflect the transfer of excitation energy between the bulk and red Chl pools in the PS-I antenna.

In all studied PS-I particles a fast 3.4- to 4.7-ps equilibration process is observed which mainly reflects energy transfer from the bulk Chls to the C708 pool of red Chls. The positive part of the spectra of this process is very similar in shape and amplitude for all PS-I cores. The negative region of the spectra appears quite similar as well, although in *Synechocystis* monomeric and trimeric PS-I this part is less pronounced than in other PS-I particles. The spectrum of the fast equilibration component is slightly non-conservative in the PS-I cores from *Synechocystis*, but it is basically conservative in the other PS-I cores, indicating that some non-equilibrium trapping occurs in the former particles, which is absent in the latter. This is consistent with the observation that the transfer component in *Synechocystis* PS-I cores is slightly slower (4.4 to 4.7 ps), than the fastest transfer component in the other PS-I particles (~3.4 to 3.9 ps).

The notion that the amount of non-equilibrium trapping increases with slower equilibration components makes of course sense, and is underlined by the spectra of the slower second equilibration processes observed in the *Synechococcus* and *Spirulina* PS-I particles (Fig. 4 *C–E*, *diamonds*), that occur on a time scale of 9.6 to 15 ps and are consequently highly non-conservative.

The spectra of the second equilibration components of *Synechococcus* trimeric and *Spirulina* monomeric and trimeric PS-I are qualitatively very similar: they exhibit a relatively large positive contribution in the blue part of the spectrum, and a red part that is only slightly negative. The maximum and width of the positive part, however, vary significantly between these three PS-I species. These differences between the DAS of the second equilibration component in monomeric and trimeric PS-I particles from *Spirulina* can be readily explained by the differences in contents of long wavelength Chls. The second transfer component involves both non-equilibrium trapping from the bulk and C708 pools and transfer from these pools to the reddest Chl pool. In monomeric PS-I from *Spirulina*, the emissions of the two long wavelength pools are spectrally less separated as compared to trimers (see below). Therefore, in monomers, the positive (decay) contribution of the emission of C708 to the spectrum of the slow transfer component is, to a certain extent, cancelled by the negative (rise) contribution of the emission of the C719 pool. This results in the slanting red wing, and the lack of a clearly negative region in the 11.6-ps DAS of the *Spirulina* monomers. In trimers the emissions of the two red pools are spectrally more separated, and consequently there is less cancellation of the emission of the C708 pool. This results in the two peaks in the positive part of the second transfer DAS in trimers, which can therefore be attributed to bulk and C708 emission. Furthermore it results in a more distinct negative region in the 15-ps DAS in trimers.

In view of the above explanation, one would expect the second equilibration DAS in *Synechococcus* trimeric PS-I to be peaking even more to the blue than *Spirulina* monomeric PS-I, because the former exhibits less C708 Chls and more C719 Chls than the latter, which would enhance the cancel-

lation effect in the red part of the spectrum. However, this is not observed. A possible explanation for this apparent discrepancy is that in *Synechococcus* trimeric PS-I more non-equilibrium trapping from the C708 Chls occurs during the second equilibration step. The C708 contribution to the second equilibration process in *Spirulina* PS-I may, in its turn, have been lowered, because some additional bulk to C708 transfer may have occurred along with the second equilibration process as well. An alternative explanation could be that the numbers and energies of the red Chls that were found from the 6-K absorption spectrum may not be valid at room temperature.

### *Trapping components*

For all PS-I particles under investigation, the slowest process is the so-called trapping component, which exhibits a DAS that is clearly positive at all wavelengths (Fig. 4 *A–E*, *triangles*). As pointed out above, the designation trapping component is somewhat misleading, as, (non-equilibrium) trapping also occurs on shorter time scales.

Both the trapping lifetime, which varies between 23 and 50 ps, and the trapping spectrum depend strongly on the numbers and energies of the red Chls, present in the various PS-I particles (Fig. 4 *A–E*, *triangles*). This pronounced correlation can easily be understood in a qualitative manner. If the excitation density distribution reflected in the trap spectrum represents a (quasi) Boltzmann equilibrium of the excitation density over the PS-I antenna Chls, the exponential Boltzmann factor will cause the equilibrium to shift rapidly to lower energies if the energies of the red states are lowered. Likewise, the number ratio in the Boltzmann factor will shift the equilibrium dependent on the number of red Chls relative to the bulk Chl*a*. The shift of the equilibrium also accounts for the observed increase in trapping lifetimes. The emission of the low energy Chls has a lower spectral overlap with the absorption of P700 than the bulk Chls (see also below). If the low energy Chls are not located exceptionally close to the RC, concentration of the excitations on these Chls will consequently result in a decreased trapping rate.

It can therefore be concluded that effectively the presence of red Chls lowers the efficiency of charge separation, but it must be noted that slowing down trapping from 20 to 50 ps only results in a decrease of the quantum yield of charge separation of 99.6 to 99.0% (assuming an intrinsic fluorescence lifetime of Chl*a* of 5 ns), which is not expected to seriously affect the organism.

We would like to point out that even though at shorter time scales energy transfer processes occur that lead to equilibration of the excitation energy throughout the antenna, this does not necessarily imply that the trap-spectrum reflects a fully Boltzmann-equilibrated distribution of excitations, but rather a so-called transfer equilibrium (Laible et al., 1994).

At this stage we have not proven that all of the differences that we observe between the different PS-I species are entirely due to the differences in red Chl contents. Below we will discuss a kinetic model to which we have fitted our data to explore, in more detail, the effects of the spectral composition of the antenna upon the experimentally observed spectral-temporal properties of the fluorescence of all PS-I species studied.

## Target analysis of the time-resolved fluorescence data: a compartmental model describing the kinetics of different PS-I core complexes

In this section the differences and similarities underlying the variation in the experimentally recorded kinetics of the various PS-I particles will be further explored.

Although the coordinates of the antenna Chls are available from the crystal structure of PS-I from *Synechococcus* (Fromme et al., 1996; Krauss et al., 1996), and this has provided important new insight into the 3-D organization of this antenna-RC complex in relation to its function, a full calculation of energy transfer in PS-I based on this structure is not straightforward. First of all, information about the orientation of the transition dipole moments of the Chls is currently missing. Second, the positions of the different Chl spectral forms are unknown. Finally, the structure is known only for *Synechococcus* PS-I. In view of the spectroscopic differences, small variations of the protein structure and Chl binding sites must be present between the different PS-I species that we have investigated, although the global organization of different PS-I species is expected to be unchanged.

Even if these difficulties are overcome by obtaining high resolution structures of the relevant proteins, relating the structure of a photosynthetic protein to spectroscopic data has proven to be very difficult, even for systems with a much smaller amount of Chls, such as, for instance, the FMO antenna complex (Savikhin et al., 1999b) or LHC II (Gradinaru et al., 1998).

Therefore we favor a relatively simple compartmental model over a structure-based calculation. This approach allows for a unified description of the dynamics in all studied PS-I cores, and generates a relatively small number of rate constants that transparently reflect the macroscopic energy transfer processes between spectrally different Chl pools. The results of this analysis allow us to quantitatively compare the various PS-I cores.

Because we chose to use discrete spectral pools, inhomogeneous broadening, allthough known to be large for the long wavelength Chls (Gobets et al., 1994; Pålsson et al., 1996), is not explicitly included in our model.

The compartmental model, presented in Fig. 5, consists of five compartments, representing the Soret state (*S*) of all spectral forms, and the $Q_y$ states of the bulk Chl pool (*B*), two red shifted Chl pools (*1* and *2*), and a pool representing

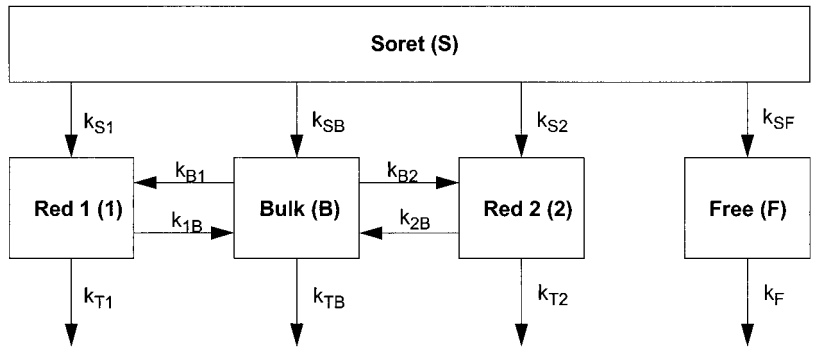


FIGURE 5 Compartmental model describing the kinetics of different cyanobacterial PS-I core particles upon excitation at 400 nm.

free Chls that are not connected to the PS-I core (*F*). For the modelling of *Synechocystis* PS-I, the second pool of red shifted Chls was omitted from the scheme.

The following rate constants were included in the model. 1) From the Soret compartment, irreversible energy transfer occurs to the three or four $Q_y$ compartments with the rate constants $k_{SB}$, $k_{S1}$, $k_{S2}$, and $k_{SF}$. The sum of these rate constants represents the observed Soret-$Q_y$ relaxation rate. The four individual rates do not have an actual physical meaning, but merely account for the initial distribution of the excitations over the different compartments, and scale with the total number of Chls in each of the pools. 2) Uphill and downhill energy transfer occurs between the red Chl compartments and the bulk Chl compartment with rate constants $k_{B1}$, $k_{B2}$, $k_{1B}$, and $k_{2B}$.

We have not included direct energy transfer between different pools of red Chls because low temperature fluorescence emission spectra of *Spirulina* trimeric PS-I indicate that energy transfer between different pools of red Chls is not very efficient (Shubin et al., 1995). Although energy transfer may occur between the two red pools in *Synechococcus* trimeric PS-I (Pålsson et al., 1996), we regard it as a secondary effect. 3) Trapping occurs from the bulk Chls with a rate constant $k_{TB,}$ and from the red Chl compartments with rate constants $k_{T1}$ and $k_{T2}$. 4) Free Chl emission decays with a rate constant $k_F$.

P700 was not included as a separate compartment in the target analysis of our data. Due to the fact that both trapping and back-transfer to the antenna occur on a sub picosecond time scale (Gobets, unpublished results), the density of excitations on P700 is very small at all times, and hence, the actual contribution of P700 to the total fluorescence is too small to be distinguished from our data.

The compartmental model was fitted to the data (target analysis), yielding the emission spectra of the different pools of Chls, as well as the rate constants that were introduced above (Holzwarth, 1996). In order to solve the model, the number of free parameters had to be reduced by fixing or manually varying some of the rate constants. The free rates were the Soret to bulk relaxation rate $k_{SB}$, the energy transfer rates $k_{B1}$, $k_{B2}$, $k_{1B}$, $k_{2B}$, and the free Chl decay rate $k_F$. Two sets of fits were generated. In the first set, the trapping rate from the bulk, $k_{TB}$, was a free parameter as well and could vary between different PS-I species. In the second set, $k_{TB}$ was fixed to $(18\ \text{ps})^{-1}$ for all species. To solve the model, a constraint had to be imposed on the emission spectra of some pools, and, therefore, the emission spectra of the low energy Chls were forced to be zero below, respectively, ~680, and ~690 nm for the first and second pool of red Chls. Because the Soret state does not fluoresce in the spectral region that was recorded, its spectrum was set to zero for all wavelengths. Some of the parameters were varied manually to meet some boundary conditions that could not be implemented directly in the target analysis. First, the Soret to $Q_y$ rates $k_{S1}$ and $k_{S2}$ were adjusted manually to $k_{SB}$ to match the initial fraction of excitations on each $Q_y$ pool to the number of Chls contained in that pool (table 1), to account for the aselective excitation. Second, we required the SAES resulting from the target analysis to have equal areas. These areas reflect the relative oscillator strength per Chl in each emitting pool, which is presupposed to be equal for all spectral forms. The areas of the spectra of the different pools were balanced by varying the trapping rates from the red Chls $k_{T1}$, $k_{T2}$, as well as the free Chl Soret to Qy relaxation rate $k_{SF}$. For some of the data-sets it was not possible to completely balance the areas of the spectra resulting from the target analysis. This problem mainly occurred for the fits in which the bulk trapping rate was fixed. In those cases we optimized the values of $k_{T1}$, $k_{T2}$, and $k_{SF}$ to get as close as possible to equal areas below the spectra. The final areas of the spectra deviated $<10\%$ from that of equal areas.

Under the constraints and conditions discussed above, the target analysis always converged to a unique optimal solution.

Due to the restrictions imposed by the model, the quality of the fit decreased slightly as compared to the analysis with parallel decaying components discussed above, which is reflected by a small increase of the root mean square error by between 2% and 8%, and some temporal and spectral

structure appearing in the residual matrix of the singular value decomposition. Nevertheless, the quality of the fit remained very good. The kinetic parameters resulting from the target analysis resulted in system lifetimes which in almost all cases deviated <10% from those found using the model with parallel decaying components (Fig. 4 and above).

### *SAES*

The SAES resulting from the target analysis of the five PS-I species are presented in Fig. 6 *A–E*. The results of the fit with a free bulk trapping rate are represented by dashed curves, and the fits for which a fixed bulk trapping rate of $(18\ \text{ps})^{-1}$ was imposed are represented by solid lines with markers. In the cases where the areas of the SAES could not be fully balanced (see above), the spectra were scaled afterwards for ease of comparison. Note that in all cases the difference between the shapes of the spectra obtained from these two different fits is negligible.

The compartment of the free Chls is in all species represented by an identical spectrum (*crosses*) that exhibits a maximum around 676 nm and shows a distinct long red tail which extends beyond the window of observation. This spectrum is very characteristic for the emission of monomeric Chl*a* in solution (Hoff and Amesz, 1991).

In all species the emission from the bulk compartment is represented by a rather characteristic shaped SAES (*squares*). We note that these bulk spectra are indistinguishable between the different PS-I species, reflecting the lack of clear differences in the dominating band of the absorption spectra. The bulk SAES exhibits a maximum around 688 nm, and shows a long red tail. Except for the 12-nm red shift, the spectrum is nearly indistinguishable from the free Chl emission spectrum.

The SAES of the C708 pool of red Chls (*triangles*) look very similar for all studied species, underpinning the strong similarity between C708 Chls contained in the PS-I cores of the different species. The maximums of these spectra all appear around 712 nm, and the spectra are considerably broader than those of the bulk Chls, reflecting the strong homogeneous and inhomogeneous broadening in these red Chl pools (Gobets et al., 1994; Pålsson et al., 1996; Rätsep et al., 2000). The similarity between the emission spectra of the C708 pools of red Chls in all PS-I species studied is striking, considering the large differences in the red parts of the 6-K absorption spectra between the different PS-I species.

Even more remarkable are the SAES of the C719 pool, occurring in *Synechococcus* PS-I trimers and *Spirulina* PS-I monomers, which are practically identical. The maximum of these spectra occurs at ~720 nm, and the width of these spectra is somewhat larger than for the first (C708) pool of red Chls, reflecting the larger (in)homogeneous broadening of these pools (Pålsson et al., 1996). The SAES of the C740

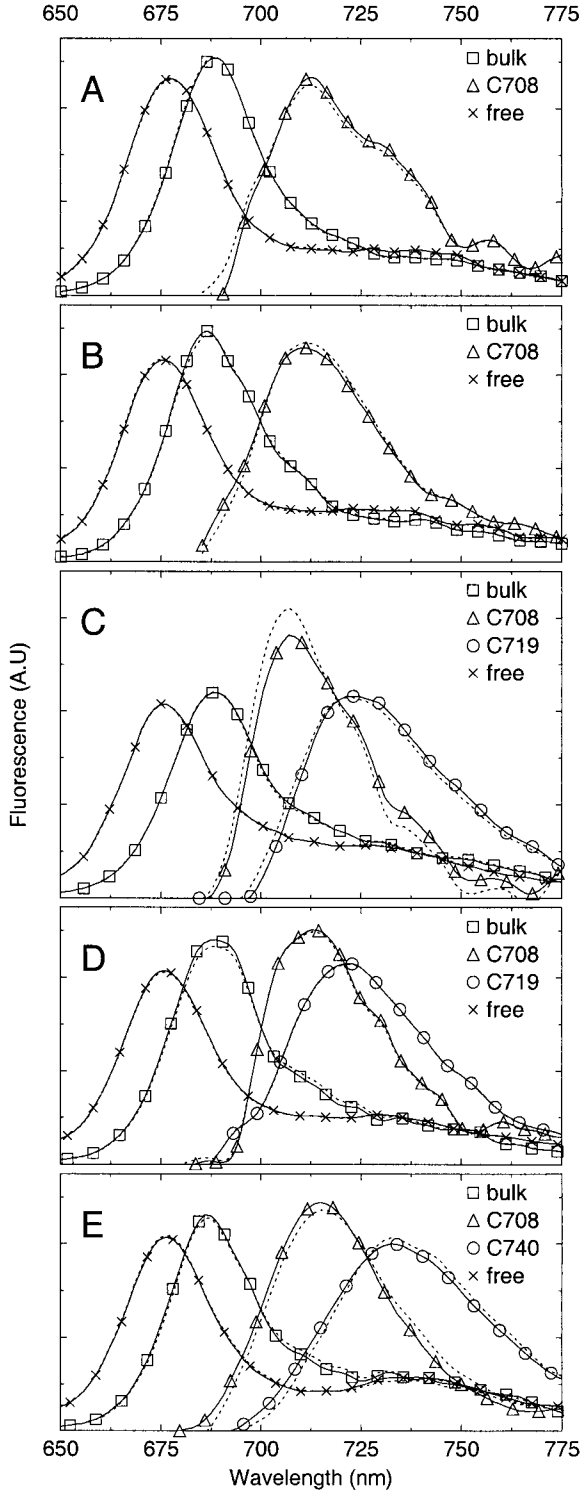


FIGURE 6 SAES of target analysis of fluorescence decay of different cyanobacterial PS-I core particles upon excitation at 400 nm. (*A*) Monomeric core of *Synechocystis sp.* PCC 6803. (*B*) Trimeric core of *Synechocystis sp.* PCC 6803. (*C*) Trimeric core of *Synechococcus elongatus*. (*D*) Monomeric core of *Spirulina platensis*. (*E*) Trimeric core of *Spirulina platensis*. *Solid lines*, the SAES of a fit for which the value of $k_{TB}$ was fixed to $(18\ \text{ps})^{-1}$; *dashed lines*, a fit for which $k_{TB}$ was a free parameter of the fit; *squares*, bulk emission; *triangles*, first red pool emission; *circles*, second red pool emission; *crosses*, free Chl emission.

pool in *Spirulina* trimers is even more red shifted, reaching a maximum at 733 nm, and the spectrum is even broader reflecting an even larger (in)homogeneous broadening of this pool.

The maximums of the room temperature emission spectra of the different pools of red Chls occur at wavelengths that are about equal to, or even shorter than, their respective 6-K absorption maximums. This remarkable feature can be explained by a significant blue shift of the absorption maximums of these red pools at room temperature (Rätsep et al., 2000).

### *Energy transfer*

The fitted values of the various rates that occur in the model (Fig. 5) are listed in table 2. Both the results of the fit with a fixed bulk trapping rate and the fit in which this rate was a free parameter of the fit are shown, the latter in parentheses.

We emphasize that the rates of energy transfer and trapping in table 2 represent effective rates. The actual values of these rates would change in case a P700 compartment could have been included in the model. However, the ratios between forward and backward rates and the ratios between the various trapping rates are hardly affected by such an additional compartment, and it is these ratios rather than the actual rates, that are important for our conclusions.

The Soret to $Q_y$ rates are not listed, because their individual values do not have a physical significance (see above). The sum of Soret to $Q_y$ rates varied between $(0.4\ \text{ps})^{-1}$ and $(0.8\ \text{ps})^{-1}$, in line with the 400- to 900-fs lifetimes found in the parallel model.

The characteristics of energy transfer between the bulk and red pools are expressed by the rates $k_{B1}$, $k_{B2}$, $k_{1B}$, and $k_{2B}$. Because the number of Chls in this first pool of (C708) Chls increases from 3 in *Synechocystis* PS-I monomers to 5 in *Synechocystis* PS-I trimers and *Synechococcus* PS-I trimers, and ~7 in *Spirulina* PS-I, the ratio $k_{B1}/k_{1B}$ is expected to increase correspondingly. The ratio $k_{B1}/k_{1B}$ does indeed follow the stoichiometry of the C708 quite well.

In the C719 pool of red Chls that appears in *Synechococcus* trimeric PSI and *Spirulina* monomeric PS-I, we find a ratio of the forward ($k_{B2}$) and backward ($k_{2B}$) rates that only differ by ~25% between these two species. This is in clear contradiction with the estimated numbers of Chls contained in this pool (4 in *Synechococcus* trimeric PS-I *versus* 1 in *Spirulina* monomeric PS-I), from which a 75% difference would be expected. These findings strongly suggest that monomeric PS-I from *Spirulina* contains more C719 Chls (and consequently less C708 Chls) at room temperature than anticipated from the Gaussian fit of the 6-K absorption spectrum.

We will use the ratio of the forward and backward energy transfer rates, and the stoichiometric estimates to calculate the energy difference between the red Chl pools and the bulk Chls, using the concept of detailed balance, which states that the energy difference between two different pools of Chls A and B can be expressed as $\Delta E = k_b T \ln(N_A k_{AB}/N_B k_{BA})$, in which $k_b$ represents Boltzmann's constant ($0.695\ \text{cm}^{-1}K^{-1}$), T the absolute temperature, $N_x$ the number of Chls in pool x, and $k_{xy}$ the transfer rate from pool *x* to pool *y*. Using the stoichiometric values from table 1 and the transfer rates from table 2, we find for the C708 pool in all studied PS-I particles a value of $\Delta$E which varies between 350 and 515 $\text{cm}^{-1}$, corresponding to a room temperature absorption maximum of this pool at around 702 nm, which corresponds well with the 702–704-nm value reported in Rätsep et al. (2000), and also seems reasonable in view of the ~712 nm emission maximum of this pool (see above), and the 10 nm Stokes' shift reported in (Gobets et al., 1994).

The energy difference of the second (C719) pool of red Chls in *Synechococcus* PS-I is found to be ~570 $\text{cm}^{-1}$, corresponding to an absorption maximum of ~708 nm. This value seems to be realistic in view of the emission maximum of this pool, which appears at 723 nm. The 11-nm blue shift of the absorption maximum of the C719 pool from 719 nm to 708 nm upon the increase of the temperature from 6 K to room temperature, is considerably larger than the 4- to 6-nm shift found for the C708 pool (Rätsep et al., 2000; see above), which indicates that the Chls in the C719 pool are more strongly coupled to their environment than those in the C708 pool.

As pointed out above we found a discrepancy between our time-resolved data, and the estimated stoichiometry of

**TABLE 2 Reciprocal of the rates from target analysis**

| Species | (Transfer rates)$^{-1}$ (ps) | | | | (Transfer rates)$^{-1}$ (ps) | | | $k_F^{-1}$ (ns) |
|---|---|---|---|---|---|---|---|---|
| | $k_{B1}$ | $k_{1B}$ | $k_{B2}$ | $k_{2B}$ | $k_{TB}$ | $k_{T1}$ | $k_{T2}$ | |
| *Synechocystis* monomers | 31 (27) | 8.6 (8.3) | | | *18* (18) | *170* (*200*) | | 4.8 (5.0) |
| *Synechocystis* trimers | 18 (20) | 8.9 (8.4) | | | *18* (17) | *38* (*63*) | | 6.7 (7.1) |
| *Synechococcus* trimers | 18 (18) | 9.3 (9.5) | 26 (22) | 17 (16) | *18* (20) | *21* (*13*) | *inf* (*inf*) | 5.3 (5.3) |
| *Spirulina* monomers | 19 (15) | 7.8 (10.2) | 43 (38) | 20 (22) | *18* (29) | *48* (*18*) | *inf* (*200*) | 5.0 (4.8) |
| *Spirulina* trimers | 15 (13) | 9.7 (12.3) | 24 (28) | 27 (30) | *18* (*27*) | *30* (*22*) | *450* (*260*) | 4.0 (4.3) |

Parameters set in italic numbers were fixed or varied manually, plain numbers indicate free-fitting parameters. Results are shown both for a fit in which the value of $k_{TB}$ was fixed to a value of $(1\delta\ \text{PS})^{-1}$ and for a fit in which $k_{TB}$ was a free fitting parameter (values in parentheses). For more details, see text.

the pools of red Chls in *Spirulina* PS-I monomers. This is also reflected by the unrealistically large value of about 800 $cm^{-1}$ for the calculated energy difference between the bulk and the second pool of red Chls in this PS-I species, if the C719 pool would consist of only one single Chl. If however we propose that instead of seven C708 and one C719 Chl, five C708 and three C719 Chls are present in *Spirulina* PS-I monomers, the calculated energy difference between the C719 and the bulk Chls pool is $\sim$575 $cm^{-1}$, corresponding to a 708-nm absorption maximum, very comparable to the value found for *Synechococcus* PS-I trimers.

The reduction of the number of C708 Chls in *Spirulina* monomers from 7 to 5 also leads to a room temperature absorption maximum at 702 nm, which is more in line with the C708 pool in the other PS-I cores (Table 1, values between parentheses).

We must therefore conclude that at room temperature the red Chl contents of *Spirulina* PS-I monomers must be very comparable to the that of *Synechococcus*, with a slightly lower amount of C719 Chls, and that the stoichiometry which was estimated from the 6 K absorption spectrum cannot be applied at room temperature for *Spirulina* monomeric PS-I. This explains the remarkable kinetic and spectral similarity between both species at room temperature, as was already mentioned in the results section.

The energy difference between the second red pool in *Spirulina* trimeric PS-I (C740) and the bulk, is about 725 $cm^{-1}$, which corresponds to an absorption maximum at 715 nm. This is a realistic value in view of the emission maximum at 733 nm. The apparent Stokes' shift of 18 nm is comparable to the 20 nm Stokes' shift found at 6 K. The blue shift of 25 nm upon a rise of the temperature from 6 K to room temperature is about five times more than found in *Synechocystis* PS-I (Rätsep et al., 2000; see above) and about two times more than found in *Synechococcus* trimeric PS-I (see above), indicating an even stronger coupling of the Chls in this extremely red shifted pool to their local environment.

### *Trapping*

If the bulk trapping rate, $k_{TB}$, is regarded as a free parameter of the fit, its value varies between $(17\ ps)^{-1}$ and $(29\ ps)^{-1}$ in the different PS-I cores. Despite this spread of values, it turns out that the quality of the fit decreases only slightly by fixing this value to $(18\ ps)^{-1}$. This common value of $k_{TB}$ had to be chosen quite close to the value found in both monomeric and trimeric PS-I from *Synechocystis* in order to obtain a good fit of the model to the results of these PS-I particles. The sensitivity of the model to the *Synechocystis* PS-I data upon varying $k_{TB}$ has two reasons. First of all, in our view, this species exhibits only one pool of red Chls, and, hence, the model for *Synechocystis* PS-I has three fewer degrees of freedom (two transfer rates and a trapping rate) than the species with two pools of red Chls. Secondly, *Synechocystis* PS-I has only very few, not very red shifted, red Chls, and, therefore, the effect that these red Chls have upon the energy transfer and trapping dynamics is relatively limited. This is illustrated by the fact that the $(18\ ps)^{-1}$ bulk trapping rate constant is quite close to the 23- to 24-ps time-constant found for *Synechocystis* PS-I in the parallel model. Modelling of the dynamics in *Synechocystis* PS-I, based on the Chl coordinates from the structure of *Synechococcus* PS-I (Gobets et al., 1998b), also showed a 18-ps trapping time upon removal of the two red Chls, which strongly suggests that this is indeed the trapping time in a bulk PS-I without red Chls.

The structure of *Synechococcus* PS-I reveals that the bulk of the antenna Chls are scattered in an ellipse around the RC. This organization defines the bulk to RC transfer rate, which in turn largely determines the effective rate of trapping $k_{TB}$ from the bulk Chls (Gobets et al., 1998b). Because the sequence homology is highly conserved between different PS-I species (Cantrell et al., 1987; Mühlenhoff et al., 1993) this organization will essentially be the same in all these species. Because also the spectral properties of the bulk and RC Chls do not vary significantly between the PS-I species investigated in this study (Fig. 1) it seems quite acceptable to propose that the bulk trapping properties are essentially the same for all PS-I species, and that in view of the discussion above, the value of this trapping rate, $k_{BT}$, should be fixed to $\sim(18\ ps)^{-1}$.

The trapping rates from any pool of antenna Chls depend in first order on the (average) distance of these Chls to P700, their relative orientation to P700, and the overlap integral of their emission spectrum with the absorption of P700. If the average location and orientation of the Chls in a red pool are not very different from the bulk Chls, the relative trapping rate from that pool as compared to the bulk Chls only depends upon the relative spectral overlap between the emission of these red Chls with the absorption of P700. At low temperatures this overlap is very small, resulting in slow trapping from the red Chls, and a low quantum efficiency of charge separation. Upon an increase of temperature the overlap increases due to a number of causes. First of all the emission (and absorption) of the strongly coupled red Chls blue shifts quite significantly, toward the absorption of P700 (Rätsep et al., 2000). Secondly, the absorption band of P700 and the emission of the red Chls broaden with increasing temperature. Finally, in the pools of red Chls, which are significantly inhomogeneously broadened at low temperatures excitations mainly reside on the lower energy Chls in the distribution, whereas at higher temperatures, the higher energy Chls in the distribution can also be excited, which results in a further blue shift of the (average) emission of the red Chls.

The room temperature trapping rates from the red Chl pools may be roughly estimated from the emission spectra found in the target analyses, and a P700 absorption spectrum, which can roughly be approximated by a Gaussian

with a FWHM of 20 nm, peaking at 698 nm (Pålsson et al., 1998). The direct trapping rates from the pools of red Chls that are calculated this way turn out to be quite significant: the direct trapping rates from the C708, C719, and C740 pools are estimated to be about 80, 30, and 15% of the bulk trapping rate, respectively. The accuracy of the smaller numbers is limited because they depend strongly upon the exact properties of the extreme blue edge of the calculated emission spectra, and because the spectral resolution of the experimental emission spectra is only 8 nm.

The trapping rates estimated this in way are comparable to the trapping rates directly resulting from the target analysis. The trapping rates $k_{T1}$ from the first pool of red Chls (C708) for the fit with the fixed bulk trapping rate $k_{TB}$ are all of the same order as $k_{TB}$, roughly matching the 80% estimate. The values of $k_{T1}$ for the fit with free bulk trapping are slightly higher, but still comparable. Monomeric PS-I of *Synechocystis* is the only exception with a value of $k_{T1}$ which is only about 10% of $k_{TB}$. It could be that the preparation of monomeric particles is heterogeneous, in the sense that some particles may contain more red Chls, and other less (or none), which results in the generally observed slightly lower red Chl content as compared to trimeric PS-I from the same species.

The trapping rates $k_{T2}$ from the second pools of red Chls measure only 10% of $k_{TB}$ or less, which is lower than the estimates indicated above. It must be noted that, in contrast to the trapping rates from the first pool of red Chls, the boundary conditions (equal spectral areas) do not depend too strongly upon these (small) trapping rates, and therefore merely represent an order of magnitude estimate.

## CONCLUSIONS

In this work we have investigated monomeric and trimeric PS-I preparations of *Synechocystis sp.* PCC 6803, *S. elongatus*, and *Sp. platensis* using room temperature time-resolved fluorescence spectroscopy. The 6-K steady state absorption spectra of these preparations reveal pronounced differences in the amounts and energies of their respective red shifted Chl forms. A C708 pool appears to be a common feature of all these particles, and a C719 pool appears in two species (*Synechococcus* trimers, *Spirulina* monomers). A C740 pool is unique for *Spirulina* PS-I trimers.

The room temperature time-resolved fluorescence measurements of these five PS-I preparations reveal a large diversity of fluorescence kinetics and spectral evolution. A fast equilibration step between the bulk Chls and the C708 pool is found to occur in ~3.5 to 5 ps in all these PS-I cores. In the species containing a second (C719 or C740) pool of red Chls, a second equilibration process along with a considerable amount of non equilibrium trapping occurs in 10 to 15 ps. Trapping from an equilibrated distribution of excitations occurs in 23 to 50 ps.

A target analysis of these data demonstrates that the kinetic and spectral differences between these particles most probably result exclusively from the differences in amounts and energies of red Chls, and that trapping from the bulk Chls may be described by a single $(18\ \text{ps})^{-1}$ rate constant.

The direct trapping rate from the C708 pool was found to be only slightly slower than trapping from the bulk Chls. Trapping from the other red pools was found to be at least an order of magnitude slower. Because the overall trapping kinetics slows down with an increase of the number of red Chls and a lowering of their energies, we conclude that increasing the trapping efficiency of the system is apparently not a function of the red Chls. The trapping rate from the bulk and C708 pools were found to be more or less proportional to the overlap between their emission spectrum and the absorption of P700. This leads us to the conclusion that the C708 Chls do not have a location very close to or far away from the reaction center, in agreement with Byrdin et al. (2000). The trapping rate from the reddest Chl pools seems to be lower than expected from the overlap-based estimate, possibly indicating a more remote location of these Chls in the structure.

Clear, well defined spectra were obtained for the different spectral forms, which show that the emission of the bulk Chls and the C708, C719, and C740 pools can also be distinguished at room temperature. The room temperature emission spectra of the red Chls are very broad and distinctly different from the bulk Chl emission spectra, reflecting that the homogeneous and/or inhomogeneous broadening of the red Chl pools are also large at room temperature.

The red Chl pools are considerably blue shifted at room temperature. C708 absorbs around 702 nm and emits around 712 nm; C719 absorbs around 708 nm and emits around 722 nm; and C740 absorbs around 715 nm and emits at 733 nm. The more red shifted a pool is, the stronger the Chls in that pool are coupled to their local environment, which is expressed by a larger temperature-dependent blue shift of this pool.

This research was supported by the Netherlands Organization for Scientific Research via the Dutch Foundation of Earth and Life Sciences (ALW), der Deutsche Forschungsgemeinschaft (Sonderforschungsbereich 480, C2 and Sonderforschungsbereich 498, TP A1), dem Fonds der Chemischen Industrie and NATO grant LST.CLG. 975955. The streak camera and amplified Ti:Sapph laser system were funded by investment grants from ALW.

## REFERENCES

Byrdin, M., I. Rimke., E. Schlodder, D. Stehlik, and T. A. Roelofs. 2000. Decay kinetics and quantum yields of fluorescence in photosystem I from *Synechococcus elongatus* with P700 in the reduced and oxidized state: are the kinetics of excited state decay trap-limited or transfer-limited? *Biophys. J.* 79:992–1007.

Cantrell, A., and D. A. Bryant. 1987. Molecular cloning and nucleotide sequence of the psaA and psaB genes of the cyanobacterium *Synechococcus* sp. *PCC* 7002. *Plant Mol. Biol*. 9:453–468.

Du, M., X. Xie, Y. Jia, L. Mets, and G. R. Fleming. 201. 1993. Direct observation of ultrafast energy transfer in PS-I core antenna. *Chem. Phys. Lett.*535–542.

Fleming, G. R., and R. van Grondelle. 1997. Femtosecond spectroscopy of photosynthetic light-harvesting systems. *Curr. Opin. Struct. Biol.* 7:738–748.

Fromme, P., and H. T. Witt. 1998. Improved isolation and crystallization of photosystem I for structural analysis. *Biochim. Biophys. Acta.* 1365: 175–184.

Fromme, P., H. T. Witt, W.-D. Schubert, O. Klukas, W. Sänger, and N. Krauss. 1996. Structure of photosystem I at 4.5 angstrom resolution: a short review including evolutionary aspects. *Biochim. Biophys. Acta.* 1275:76–83.

Gobets, B., J. P. Dekker, and R. van Grondelle. 1998a. Transfer-to-the-trap limited model of energy transfer in photosystem I. *In* Photosynthesis: Mechanisms and Effects. Vol. 1. G. Garab, editor. Kluwer Academic Publishers, Dordrecht, The Netherlands. 503–508.

Gobets, B., H. van Amerongen, R. Monshouwer, J. Kruip, M. Rögner, R. van Grondelle, and J. P. Dekker. 1994. Polarized site-selected fluorescence spectroscopy of isolated photosystem I particles. *Biochim. Biophys. Acta.* 1188:75–85.

Gobets, B., I. H. M. van Stokkum, F. van Mourik, M. Rögner, J. Kruip, J. P. Dekker, and R. van Grondelle. 1998b. Time-resolved fluorescence measurements of photosystem I from *Synechocystis* PCC 6803. *In* Photosynthesis: Mechanisms and effects. Vol. 1. G. Garab, editor. *Kluwer Academic Publishers, Dordrecht, The Netherlands*. 571–574.

Gradinaru, C. C., S. Ozdemir, D. Gulen, I. H. M. van Stokkum, R. van Grondelle, and H. van Amerongen. 1998. The flow of excitation energy in LHCII monomers: Implications for the structural model of the major plant antenna. *Biophys. J.* 75:3064–3077.

Greene, B. J., and R. C. Farrow. 1983. The subpicosecond kerr effect in $CS_2$. *Chem. Phys. Lett.* 98:273–276.

Hastings, G., F. A. M. Kleinherenbrink, S. Lin, and R. E. Blankenship. 1994. Time-resolved fluorescence and absorption-spectroscopy of photosystem-I. *Biochemistry* 33:3185–3192.

Hastings, G., L. J. Reed, S. Lin, and R. E. Blankenship. 1995. Excited state dynamics in photosystem I: effects of detergent and excitation wavelength. *Biophys. J.* 69:2044–2055.

Hayes, J. M., S. Matsuzaki, M. Rätsep, and G. J. Small. 2000. Red chlorophyll *a* antenna states of photosystem I of the cyanobacterium *Synechocystis* sp. *PCC* 6803. *J. Phys. Chem. B.* 5625–5633.

Hoff, A. J., and J. Amesz. 1991. Visible absorption spectroscopy of chlorophylls. *In* Chlorophylls. H. Scheer, editor. CRC Press, Boca Raton, FL. 723–738

Hoff, W. D., I. H. M. van Stokkum, H. J. van Ramesdonk, M. E. van Brederode, A. M. Brouwer, J. C. Fitch, T. E. Meyer, R. van Grondelle, and K. J. Hellingwerf. 1994. Measurement and global analysis of the absorbance changes in the photocycle of the photoactive yellow protein from Ectothiorhodospira halophila. *Biophys. J.* 67:1691–1705.

Holzwarth, A. R. 1996. Data analysis of time-resolved measurements. *In* Biophysical Techniques in Photosynthesis. J. Amesz, and A. J. Hoff, editors. Kluwer, Dordrecht, the Netherlands. 75–92.

Holzwarth, A. R., G. Schatz, H. Brock, and E. Bittersmann. 1993. Energy transfer and charge separation kinetics in photosystem I. Part 1: Picosecond transient absorption and fluorescence study of cyanobaterial photosystem I particles. *Biophys. J.* 64:1813–1826.

Karapetyan, N. V., D. Dorra, G. Schweitzer, I. N. Bezsmertnaya, and A. R. Holzwarth. 1997. Fluorescence spectroscopy of the longwave chlorophylls in trimeric and monomeric photosystem I core complexes from the cyanobacterium *Spirulina platensis. Biochemistry.* 36:13830–13837.

Karapetyan, N. V., A. R. Holzwarth, and M. Rögner. 1999. The photosystem I trimer of cyanobacteria: molecular organization, excitation dynamics and physiological significance. *FEBS Lett.* 460:395–400.

Kennis, J. T. M., B. Gobets, I. H. M. van Stokkum, J. P. Dekker, R. van Grondelle, and G. R. Fleming. 2001. Light harvesting by chlorophylls and carotenoids in the photosystem I complex of *Synechococcus elongatus*: a fluorescence up-conversion study. *J. Phys. Chem. B.* 105: 4485–4494.

Klukas, O., W. D. Schubert, P. Jordan, N. Krauss, P. Fromme, H. T. Witt, and W. Saenger. 1999. Localization of two phylloquinones, Q(K) and Q(K)', in an improved electron density map of photosystem I at 4-angstrom resolution. *J. Biol. Chem.* 274:7361–7367.

Krauss, N., W.-D. Schubert, O. Klukas, P. Fromme, H. T. Witt, and W. Saenger. 1996. Photosystem I at 4-Å resolution represents the first structural model of a joint photosynthetic reaction center and core antenna system. *Nat. Struct. Biol.* 3:965–973.

Kruip, J., D. Bald, E. Boekema, and M. Rögner. 1994. Evidence for the excistence of trimeric and monomeric photosystem I complexes in thylakoid membranes from cyanobacteria. *Photosynth. Res.* 40: 279–286.

Kruip, J., E. J. Boekema, D. Bald, A. F. Boonstra, and M. Rögner. 1993. Isolation and structural characterization of monomeric and trimeric photosystem-I complexes ($P700\text{-}F_a/F_b$ and $P700\text{-}F_x$) from the cyanobacterium *Synechocystis* PCC-6803. *J. Biol. Chem.* 268:23353–23360.

Kruip, J., N. V. Karapetyan, IV Terekhova, and M. Rögner. 1999. In vitro oligomerization of a membrane protein complex. *J. Biol. Chem.* 274: 18181–18188.

Laible, P. D., W. Zipfel, and T. G. Owens. 1994. Excited-state dynamics in chlorophyll-based antennae: the role of transfer equilibrium. *Biophys. J.* 66:844–860.

Limantara, L., R. Fujii, J. P. Zhang, T. Kakuno, H. Hara, A. Kawamori, T. Yagura, R. J. Cogdell, and Y. Koyama. 1998. Generation of triplet and cation-radical bacteriochlorophyll a in carotenoidless LH1 and LH2 antenna complexes from Rhodobacter sphaeroides. *Biochemistry* 37: 17469–17486.

Melkozernov, A. N., S. Lin, and R. E. Blankenship. 2000. Excitation dynamics and heterogeneity of energy equilibration in the core antenna of photosystem I from the cyanobacterium *Synechocystis* sp. *PCC* 6803. *Biochemistry.* 39:1489–1498.

Mühlenhoff, U., W. Haehnel, H. Witt, and R. G. Herrmann. 1993. Genes encoding 11 subunits of photosystem I from the thermophilic cyanobacterium *Synechococcus* sp. *Gene.* 127:71–78.

Pålsson, L.-O., J. P. Dekker, E. Schlodder, R. Monshouwer, and R. van Grondelle. 1996. Polarized site-selective fluorescence spectroscopy of the long-wavelength emitting chlorophylls in isolated photosystem I particles of *Synechococcus elongatus. Photosynth. Res.* 48:239–246.

Pålsson, L.-O., C. Flemming, B. Gobets, R. van Grondelle, J. P. Dekker, and E. Schlodder. 1998. Energy transfer and charge separation in photosystem I: P700 oxidation upon selective excitation of the long-wavelength chlorophylls of *Synechococcus elongatus. Biophys. J.* 74: 2611–2622.

Pålsson, L.-O., S. E. Tjus, B. Andersson, and T. Gillbro. 1995. Energy-transfer in photosystem-I: time-resolved fluorescence of the native photosystem-I complex and its core complex. *Chem. Phys.* 194:291–302.

Peterman, E. J. G., S. O. Wenk, T. Pullerits, L.-O. Pålsson, R. van Grondelle, J. P. Dekker, M. Rögner, and H. van Amerongen. 1998. Fluorescence and absorption spectroscopy of the weakly fluorescent chlorophyll *a* in cytochrome b(6)f of *Synechocystis* PCC6803. *Biophys. J.* 75:389–398.

Rätsep, M., T. W. Johnson, P. R. Chitnis, and G. J. Small. 2000. The red-absorbing chlorophyll a antenna states of photosystem I: a hole-burning study of *Synechocystis* sp PCC 6803 and its mutants. *J Phys. Chem. B* 104:836–847.

Savikhin, S., D. R. Buck, and W. S. Struve. 1999b. The Fenna-Matthews-Olson protein: a strongly coupled photosynthetic antenna. *In* Resonance Energy Transfer. D.L. Andrews, and A.A. Demidov, editors. John Wiley and Sons, Inc., New York. 399–434.

Savikhin, S., W. Xu, V. Soukoulis, P. R. Chitnis, and W. S. Struve. 1999a. Ultrafast primary processes in photosystem I of the cyanobacterium *Synechocystis sp.* PCC *6803. Biophys. J.* 76:3278–3288.

Schubert, W.-D., O. Klukas, N. Krauss, W. Saenger, P. Fromme, and H. T. Witt. 1997. Photosystem I of *Synechococcus elongatus* at 4 angstrom resolution: comprehensive structure analysis. *J. Mol. Biol.* 272:741–769.

Shubin, V. V., S. D. S. Murthy, N. V. Karapetyan, and P. Mohanty. 1991. Origin of the 77K variable fluorescence at 758 nm in the cyanobacterium *Spirulina platensis. Biochim. Biophys. Acta.* 1060:28–36.

Shubin, V. V., I. N. Bezsmertnaya, and N. V. Karapetyan. 1992. Isolation from *Spirulina* membranes of two photosystem I-type complexes, one of which contains chlorophyll responsible for the 77 K fluorescence at 760 nm. *FEBS Lett.* 309:340–342.

Shubin, V. V., I. N. Bezsmertnaya, and N. V. Karapetyan. 1995. Efficient energy-transfer from the long-wavelength antenna chlorophylls to P700 in photosystem-I complexes from *Spirulina platensis. J. Photochem. Photobiol. B.* 30:153–160.

Trinkunas, G., and A. R. Holzwarth. 1994. Kinetic modeling of exciton migration in photosynthetic systems. 2. simulations of excitation dynamics in 2-dimensional photosystem core antenna/reaction center complexes. *Biophys. J.* 66:415–429.

Trissl, H.-W., B. Hecks., and K. Wulf. 1993. Invariable trapping times in photosystem-I upon excitation of minor long-wavelength-absorbing pigments. *Photochem. Photobiol.* 57:108–112.

Turconi, S., J. Kruip, G. Schweitzer, M. Rögner, and A. R. Holzwarth. 1996. A comparitive fluorescence kinetics study of photosystem I monomers and trimers from *Synechocystis* PCC 6803. *Photosynth. Res.* 49: 263–268.

Turconi, S., G. Schweitzer, and A. R. Holzwarth. 1993. Temperature dependence of picosecond fluorescence kinetics of a cyanobacterial photosystem I particle. *Photochem. Photobiol.* 57:113–119.

Valkunas, L., G. Trinkunas, V. Liuolia, and R. van Grondelle. 1995. Nonlinear annihilation of excitations in photosynthetic systems. *Biophys. J.* 69:1117–1129.

van Grondelle, R. 1985. Excitation energy transfer, trapping and annihilation in photosynthetic systems. *Biochim. Biophys. Acta.* 811:147–195.

van Grondelle, R., J. P. Dekker, T. Gillbro, and V. Sundström. 1994. Energy transfer and trapping in photosynthesis. *Biochim. Biophys. Acta.* 1187:1–65.

van der Lee, J., D. Bald, S. L. S. Kwa, R. van Grondelle, M. Rögner, and J. P. Dekker. 1993. Steady-state polarized-light spectroscopy of isolated photosystem-I complexes. *Photosynth. Res.* 35:311–321.

Wittmerhaus, B. P., V. M. Woolf, and W. F. J. Vermaas. 1992. Temperature dependence and polarization of fluorescence from photosystem I in the cyanobacterium *Synechocystis sp* PCC 6803. *Photosynth. Res.* 31: 75–87.